STUDY OF WATERFLOODING PROCESS IN NATURALLY FRACTURED RESERVOIRS FROM STATIC AND DYNAMIC IMBIBITION EXPERIMENTS

Erwinsyah Putra, Yan Fidra, ITB/New Mexico of Mining and Technology and David S. Schechter, New Mexico PRRC

Abstract

Imbibition plays an important role in oil recovery from the naturally fractured Spraberry Trend Area. Therefore, understanding matrix-fracture transfer and the key parameters associated with the imbibition process are important. We examined these issues by performing static and dynamic imbibition experiments. Oil recoveries from both experiments were matched and the imbibition processes were investigated by developing a numerical finite difference scheme and utilizing a commercial simulator.

Static imbibition experiments, followed by waterflooding, were performed at reservoir conditions to investigate rock wettability. A two-phase and 2-D, fully finite-difference implicit scheme was developed to solve non-linear diffusion in the static imbibition equation. The numerical results that matched satisfactorily with the spontaneous imbibition data were applied to investigate the effect of key variables on the imbibition rate. We found that the measurement of Amott wettability index and the capillary pressure result suggested that the Spraberry rock matrix is weakly water-wet.

Dynamic imbibition experiments were performed using artificially fractured Berea and Spraberry cores at reservoir conditions to illustrate the actual process of waterflooding in naturally fractured reservoirs. A commercial numerical simulator was used to match these experiments to generate matrix capillary pressures. A comparison between capillary pressures obtained from both experiments has been made. The results of this study were also used to determine the critical injection rate. The critical injection rate from core dimensions was upscaled to field dimensions using a dimensionless equation. Knowledge of the critical injection rate is useful in solving the problem of early breakthrough, one of the hazards of water injection in naturally fractured reservoirs.

The results of these two studies, static and dynamic imbibitions, provide useful guidelines for reservoir simulation field development in naturally fractured reservoirs.

Static imbibition experiments

Imbibition plays an important role in the recovery of oil from the naturally fractured Spraberry area. Imbibition describes the rate of mass transfer between the rock and the fractures. Therefore, understanding the imbibition process and the key parameters that control the imbibition process are crucial. Several studies have been conducted to simulate spontaneous imbibition in a core plug. These studies were concerned primarily with capillary pressure as the only driving force in the spontaneous imbibition process.[1-5]

In order to understand the physical process of imbibition, the spontaneous imbibition experiments were performed using the imbibition apparatus schematically shown in **Fig. 1**. As can be seen from the figure, the apparatus is basically a simple glass container equipped with a graduated glass cap. To perform an imbibition test, a core sample was immersed in the glass container filled with preheated brine solution. The container was then covered with the graduated cap. After fully filling the cap with brine solution, the container was then stored in an air bath that had been set at a constant temperature of 138^{o}F.

Synthetic Spraberry brine and Spraberry dead oil were used in the experiments. The brine contains NaCl and $CaCl_2.H_2O$ mixed with distilled water. Viscosity was determined using a Cannon-Fenske routine viscometer and density was determined using a digital density meter. The interfacial tensions (IFTs) of the oil/brine systems were measured using a pendant drop instrument and a de Nouy Ring. The viscosity, density and IFT of the synthetic brine and Spraberry dead oil measured at elevated temperature were tabulated in **Table - 1**.

Due to capillary imbibition action, oil was displaced from the core sample by the imbibing brine. The displaced oil accumulated in the graduated cap by gravity segregation. During the experiment, the volume of produced oil was recorded against time. Before taking the oil volume reading, the glass container was gently shaken to expel oil drops adhering to the core surface and the lower part of the cap, so that all of the produced oil accumulated in the graduated portion of the glass cap. At an early stage of the test the oil volume was recorded every half-hour while toward the end of the test the oil volume reading was made every 24 hours. Excluding the core preparation, one series of tests was usually completed within 21 days. After spontaneous imbibition in brine was completed, the core sample was subjected to forced displacement by water using a pressure ranging from 120 to 200 psi depending on the wetting condition. The injections were performed under reservoir conditions. Once the imbibition test was stopped, the core was flushed by preheated brine right away. The amount of oil produced was used to determine the wettability index for water (I_w).

Static imbibition modeling

We realize that spontaneous imbibition experiments usually takes a long time, especially when we need to vary some parameters to investigate their effects on the imbibition rate. Sometimes may be very difficult to determine capillary pressure and to illustrate water saturation profiles at different times and locations. Therefore, numerical modeling is needed to simulate this process.

In order to describe the spontaneous imbibition process, mathematical formulation for that process was derived. In deriving the governing equation, some assumptions are used; gravity terms are negligible, capillary pressure is the only driving force where total velocity is zero, and fluid and rock are incompressible. By using the simultaneous flow of two-phase formulation the governing equation for describing the spontaneous imbibition process can be obtained as follows (Chen *et al.*, 1995)[5]:

$$\nabla \cdot D(S_w) \frac{\partial S_w}{\partial x} = -f \frac{\partial S_w}{\partial t} \quad \text{.....(1)}$$

where the non-linear capillary diffusion coefficient is defined as

$$D(S_w) = \frac{k}{m_o} k_{ro} f_w \frac{\partial p_c}{\partial S_w} \quad \text{.....(2)}$$

where water fractional flow is defined as

$$f_w = \left(1 + \frac{k_{ro}}{m_o} \frac{m_w}{k_{rw}}\right)^{-1} \quad \text{.....(3)}$$

Because of the non-linear capillary diffusion coefficient, Eq. 1 was solved by numerical methods.

In order to solve it numerically, Eq. 1 was discretized in 2D finite-difference form. The left-hand side was discretized by applying the Taylor series using central difference and the right-hand side using backward difference. Note that the relative permeabilities and capillary pressure are functions of water saturation, thus, Eq. 1 must be solved iteratively. Once the new saturations are solved using the initial guess, these new water saturations are compared with the old water saturations until acceptable convergence has been reached.

The core plug is totally immersed in the water and therefore, boundary conditions are set to be 1-S_{or}. This implies that instantaneous imbibition occurs at the matrix-fracture interface. Initial conditions are required to begin the time step sequence. In this study, initial conditions are specified equal to initial water saturation.

In order to match the recovery from the imbibition experiments, only capillary pressure was altered and other parameters were kept constant. The following relative permeability correlations from Honarpour *et al* (1986)[6] were used as inputs:

$$k_{ro} = k_{ro}^{o}(1 - S_w^*)^3 \quad \text{.....(4)}$$

$$k_{rw} = k_{rw}^{o}(S_w^*)^3 \quad \text{.....(5)}$$

For the base case, the maximum oil relative permeability (k_{ro}^{o}) was set to 1.0 and the maximum water relative permeability (k_{rw}^{o}) was set to 0.3. In these relationships, the S_w* is expressed as $S_w^* = \frac{(S_w - S_{wi})}{(1 - S_{or} - S_{wi})}$. The residual oil saturation (S_{or}) was set to 0.5437 and irreducible water saturation (S_{wi}) was set to 0.37. Those average values of S_{or} and S_{wi} values are obtained from **Table 1**.

Dynamic imbibition experiments

The capillary force is the only force to recover oil during static imbibition tests. However, there are two processes involved during producing oil by waterflooding in naturally fractured reservoirs, spontaneous imbibition (capillary force) and displacement processes (viscous force). During spontaneous imbibition, water imbibes into the matrix and oil is expelled from the matrix to the fracture (counter current mechanism). The oil that reaches the fracture is displaced by injected water to the production end of the fracture, as shown in **Fig. 2**. Several laboratory and numerical studies have been conducted regarding this subject.[7-11]

In order to understand the imbibition process in an artificially fractured core, a coreflood experiment at low water injection rate was performed at reservoir temperature. A low-permeability Berea core sample was cut in cylindrical shape, 3 in. long and 1.5 in. diameter. The fracture pattern on the core sample was generated along the long axis using a hydraulic cutter. The cut sections were put back together without polishing the cut surfaces and without spacers. Synthetic Spraberry brine and Spraberry crude oil were used as wetting and non-wetting phases. The properties of rock and fluids for both cores used in this experiment are shown on **Tables 2 and 3**.

In general, the experimental process was started by saturating the core sample with 100% Spraberry oil. This process was followed by brine imbibition flooding as the wetting phase. The experimental procedure is described in detail as follows:

- Dimension of core sample was measured and then weighed.
- Core sample was inserted into a Hassler-type core holder using a confining pressure of 500 psi to saturate the core by oil. About 2-5 PV of Spraberry crude oil were passed through the core sample using the constant pressure of 30 psi supplied by a nitrogen tank. Then, the volume of oil produced was measured to determine the oil rate. By using Darcy's law, the absolute matrix permeability to oil was then calculated.
- After permeability measurement, oil-saturated core was taken from the core holder and covered with aluminum foil to prevent air penetration into the core sample. Then, it was cut in half using a hydraulic cutter to generate fracture horizontally along the axis of the core. The oil-saturated artificially fractured core was then weighed to determine core pore volume and porosity.
- The core was inserted back into the Hassler-type core holder. The effective permeability of the fractured core was determined by injecting oil into fractured core in the core holder. The fracture permeability (Guo and Svec, 1998)[12] was calculated based on the following equation by assuming the fracture porosity of 1%:

$$k_e = k_m + f_f k_f \quad \text{.....(6)}$$

where k_e(mD), k_m(mD) k_f(mD)and f_f(fraction) are the effective reservoir permeability, matrix permeability, fracture permeability and fracture porosity, respectively.

The fracture width, w_f(cm), was calculated based on the correlation developed by Seright *et al* (1996)[13]:

$$w_f = 0.000131\sqrt{k_f} \quad \text{.....(7)}$$

- The oil-saturated artificially fractured core was taken again from the core holder to clean oil from the core surface. Then, the core was inserted back into the core holder to start the experiment. The face of the matrix was sealed off by wrapping plastic and aluminum foil, in order to allow brine injection flow only through the fracture. This set-up was stored in an air bath with constant temperature of 138°F, as shown in **Fig. 3**.
- During the experiment, the oil-saturated core sample was flooded by injecting synthetic Spraberry brine into the fracture with constant brine injection rate of 4.0 cc/hour. The oil and brine produced were collected against time at the producing end of the fractured core for about 48 hours, until zero oil production-rate was achieved.

Dynamic imbibition modeling

Single porosity simulation was used instead of dual porosity simulation, because single porosity is more representative for modeling a single fracture from the artificially fractured core. However, this single porosity simulation has to be able to duplicate the behavior of dual porosity simulation, which has different properties for matrix and fracture media. Thus, the properties of a fracture should be added in the single porosity simulator, such as porosity, permeability, relative permeability, and capillary pressure.

The rectangular grid block was used to overcome the difficulty of modeling the cylindrical core shape. The pore volume of the rectangular shape was set to be the same as the cylindrical core pore volume. Three layers were used in the model with the fracture layer between the matrix layers. In addition, 10 x 10 grid blocks were used in x and y direction. The fracture layer was injected at one end with low constant water injection rate of 4.0 cc/hour (Berea core). Oil and water were produced at the opposite end of the fracture layer. The rest of the boundary blocks had a specified no-flow boundary condition.

Relative permeability for the matrix layer was calculated from the following relationships (Kazemi and Merrill, 1977).[14]

$$k_{rw} = S_w^{\,3} \quad \text{.....(8)}$$

$$k_{ro} = (S_o - S_{or})^3 \quad \text{.....(9)}$$

while relative permeability for the fracture layer was assumed to be a straight line for both k_{rw} and k_{ro}.

Similar procedures were carried out with the Spraberry core, except for using a more refined grid block in the vertical direction and Spraberry relative permeability curves (**Fig. 4**). The refined grid block was used to avoid numerical instability because the grid blocks representing the fracture are very small and the matrix permeability is very low (0.1 md) compared to that of Berea core (28.09 md). As with the Berea core, relative permeability was fixed and the main adjusted parameter was the matrix capillary pressure. Zero capillary pressure was used as the base case in fracture layer for both Berea and Spraberry cores.

The initial condition from the reservoir simulator is obtained from the hydrostatic equilibrium calculation. For instance, initial water saturation is determined by capillary pressure, which is based on the difference between oil pressure and water pressure. Thus, it is difficult to use the equilibrium option to represent initial conditions for the laboratory experiment. Instead of using the equilibrium option, initial water saturation and pressure were input directly, since those initials were known from laboratory experiments.

Results and Discussion

The average of residual oil saturations after spontaneous imbibition experiments was still very high. Therefore, the water saturation changes during the simulation are very small, which causes the numerical solution to become unstable and the result cannot be obtained. In order to approach this problem, three lower residual oil saturations of 0.2, 0.3 and 0.4 were used. Once the numerical solution matched with the experimental data, the matrix capillary pressures from different residual oil saturations were obtained. Then, the matrix capillary pressure for 0.54 residual oil saturation was estimated as shown in **Fig. 5**. The low-capillary pressure curve obtained indicates that the Spraberry cores are weakly water-wet. The weakly water-wet indication is also found by the measurement of wettability index (average Amott index is 0.3).

Figure 6 shows four experimental data and numerical solution matches for recovery against time using residual oil saturation of 0.2. The diffusion coefficient as shown in Eq. 2 is strongly non-linear due to varying capillary pressure and relative permeability curves as functions of water saturation. Therefore, using constant capillary pressure and relative permeability curves to solve the spontaneous imbibition equation, which is always solved by analytical solution, may fail to predict oil recovery by spontaneous imbibition.

Sensitivity studies on imbibition rate for varying capillary pressure, oil and water relative permeability curves, oil and water viscosity, and initial water saturation were conducted using 0.2 S_{or} case. The numerical results using the value from **Table 2** show that increasing and decreasing the value of water viscosity and water relative permeability have no effect on the imbibition rate.

In numerical modeling of the dynamic imbibition process, the matrix capillary pressure controlling the imbibition mechanism was the primary parameter adjusted to match the experimental data. Meanwhile, the fracture capillary pressure was set to be zero. The cumulative water production, oil production rate, cumulative oil production, oil recovery and water cut were parameters used to match between the observed experimental data and the numerical model. The best matches between experimental data and numerical solution (only cumulative water production and cumulative oil production are presented) can be seen in the **Figs. 7** through **10**.

The cumulative water production of Berea core shows that once brine injection was started with a constant rate of 4.0 cc/hr, oil was produced simultaneously. However, the water still was not produced. This indicated that the water was imbibing into the rock and oil was expelled from the matrix to the fracture. After two hours of brine injection, the water breakthrough was occurred because the maximum of matrix capillary pressure was reached. Consequently, water started to produce before being completely imbibed. Water was produced until 100% watercut was reached. Similar behavior was also shown by the performance of cumulative water production of Spraberry core.

The matrix capillary pressures for Berea and Spraberry cores generated, after matching was obtained, are shown in **Fig. 11**. Although matrix capillary pressure for Berea core is lower than for Spraberry core, oil recovery for Berea core is higher than for Spraberry core. The higher cumulative oil production is because of capillary imbibition transfer for Berea core is higher than for Spraberry core.

In naturally fractured reservoirs, fluid displacement in fracture network occurs due to its higher conductivity compared to the matrix while an exchange of fluids occurs between matrix and fracture system. The fluid transfer process is controlled by flow of water under naturally imposed pressure gradients (viscous force) and the spontaneous movement of water into the matrix under capillary forces (imbibition). The parameters that affect this process can be grouped into a dimensionless equation, called the fracture capillary number. This equation is used to determine the critical injection rate and is defined as the ratio between the viscous force that is parallel to the fracture direction and the capillary force that is perpendicular to the fracture direction. The viscous force is defined as a function of water velocity, water viscosity and fracture volume and is assumed to occur only in the fracture. The capillary force that occurs only in the matrix is defined as a function of interfacial tension, contact angle and matrix volume. Thus, the fracture capillary number can be written below:

$$N_{f_{VC}} = \frac{Viscous\ Force}{Capillary\ Force} = \frac{n\, m_w\, A_f}{s\ cosq\ A_m} \quad \text{.....(10)}$$

Rearranging this equation, it can be rewritten as follows:

$$N_{f_{VC}} = \frac{q_{inj} m_w}{\frac{Pc,max}{J(swi)} \sqrt{\frac{k_m}{f_m}} A_m} \quad \text{.....(11)}$$

For the lab units, the Eq. 4.6 can be written as

$$N_{f_{VC}} = \frac{1.27 * 10^{-5} * q_{inj}(cc/hr) m_w(cp)}{\frac{Pc,max(psi)}{J(swi)} \sqrt{\frac{k_m(md)}{f_m}} A_m(cm^2)} \quad \text{.....(12)}$$

Using similar manner, the lab units can be scaled to field units as written below:

$$N_{f_{VC}} = \frac{9.05 * 10^{-5} * q_{inj}(STB/Day) m_w(cp)}{\frac{Pc,max(psi)}{J(swi)} \sqrt{\frac{k_m(md)}{f_m}} A_m(ft^2)} \quad \text{.....(13)}$$

Five different injection rates of 2.0, 4.0, 8.0, 16.0, and 40.0 cc/hr were applied in the artificially fractured Berea core and three different injection rates of 0.2, 0.5, and 1.0 cc/hr were applied in the artificially fractured Spraberry core to determine the critical injection rate. The cumulative oil production at zero production rate from different injection rates was recorded and plotted in the form of injection rate against the ratio between total oil produced and total fluid produced (TOP/TFP), or called an oil cut as shown in **Fig. 12**. The results show that the oil cut produced from Berea core is higher than that from Spraberry core. This is mainly because Berea core has higher permeability (63 md) than Spraberry core (0.1 md).

At lower 2.0 cc/hr injection rates performed at fractured Berea core, the capillary force (static imbibition mechanism) was the only force in the coreflooding process. Thus, oil recovery took a long time. When using the injection rate between 2.0 and 20.0 cc/hr, both capillary pressure and viscous forces were dominant (dynamic imbibition mechanism). This means that when water imbibed into the matrix and released oil from the matrix to the fracture by capillary force, oil stored in the fracture was pushed by viscous forces, depending on volume of water injected. However, at a higher injection rate (more than 20 cc/hr), coreflooding was inefficient process because the viscous force was the only dominant mechanism. After the maximum of capillary pressure was reached, the producing end produced only water. Thus the oil cuts from 20 cc/hr injection rate were about the same as the oil cut using 40 cc/hr. However, the cost of using 40 cc/hr injection rate is much expensive because more water was injected than with the 20 cc/hr injection rate. The results also suggest that the critical injection rate, which is defined as the maximum injection rate in which the capillary and viscous forces are still dominant, can be determined at 20 cc/hr.

In order to upscale to field dimensions, Eq. 12 and the rock properties of Berea and Spraberry cores (**Table 4**) were used. The injection rate of 20 cc/hr from Berea core was converted to N_{fvc} of 2.82 x 10^{-7}. Using this N_{fvc} number, the critical injection rate for the field dimension can be recalculated using Eq. 13. We found that by upscaling to the 40- and 80-acre field dimensions, the critical injection rates are 1013 and 1433 STB/D, respectively. Similar for the Spraberry core, we found that critical injection rates for 40-acre and 80-acre field dimensions are 393 and 556 STB/D, respectively.

Conclusions

1. Low imbibition capillary pressure was generated from the model in order to match the experimental data. Laboratory experiments indicate that the wettability of the core plug was weakly water-wet.

2. An effective capillary pressure curve can be obtained from dynamic imbibition experiments by matching the recovery curves from experimental data and numerical simulation.
3. The matrix capillary pressure indicates that the wettability of Berea core is more water-wet than that of Spraberry core, even though Spraberry has much smaller pore throat sizes. Thus, imbibition capillary pressure is more dominant in Berea core than in Spraberry core.
4. The imbibition transfer is more effective for low injection rates due to lower viscous forces and longer contact time with the matrix.
5. The critical injection rate depends on the properties of the rock. Critical injection rate for Berea core in lab and 80-acre field dimensions is 20 cc/hr and 1433 STB/D, respectively. That for Spraberry core is 10.0 cc/hr and 556 STB/D, respectively.

Nomenclature

A = area, L^2
dy = length of the core in y-direction, L
dz = height of the core, L
D = capillary diffusion coefficient, ML^3T^{-2}
f = fractional flow, dimensionless
$J(S_{wi})$ = J-function at S_{wi}, dimensionless
k = permeability, L^2
k_r = relative permeability, dimensionless
$P_{c,max}$ = maximum capillary pressure, $ML^{-1}T^{-2}$
q_{inj} = volumetric injection rate, L^3T^{-1}
S = saturation, fraction
t = time, T
v = velocity of the injected fluid in the fracture, LT^{-1}
w = fracture width, L
x = spatial coordinate, L

Greek letters

s = interfacial tension, MT^{-2}
q = contact angle, degree
f = fracture porosity, fraction
m = viscosity, $ML^{-1}T^{-1}$

Subscripts

e = effective
f = fracture
i = initial
m = matrix
o = oil
r = residual
w = water

References

1. Baker, R and Wilson, G.: " Numerical Simulation of Laboratory Scale Imbibition Experiment," Internal Report Epic Consultant Services Ltd., (April 1997).
2. Bech, N., Jensen, O.K. and Nielsen, B.: "Modeling of Gravity-Imbibition and Gravity-Drainage Processes," *SPERE* (Feb. 1991) 129-136.

3. Beckner, B. L., Ishimoto, K., Yamaguchi, S., A. Firoozabadi and Azis, K.: "Imbibition-Dominated Matrix-Fracture Fluid Transfer in Dual Porosity Simulators," paper SPE 16981 presented at the 1987 SPE Annual Technical Conference and Exhibition, Dallas, TX., Sept. 27-30.
4. Blair, P.M.: "Calculation of Oil Displacement by Countercurrent water Imbibition," *SPEJ*, Sept. 1964, 195-202; *Trans.*, AIME, **231**.
5. Chen, J., Miller, M.A. and Sepehrnoori, K.: "Theoretical Investigation of Countercurrent Imbibition in Fractured Reservoir Matrix Blocks," paper SPE 29141 presented at the 1995 symposium on reservoir simulation, San Antonio, TX., Feb. 12-15.
6. Honarpour, M., Koederitz, L. and Harvey, A. H.: Relative Permeability of Petroleum Reservoirs, CRC Press, Inc., Boca Raton, FL, (1986).
7. Brownscobe, E.R. and Dyes, A.B.: "Water-Imbibition Displacement-A Possibility for the Spraberry," *Drill. and Prod. Prac.* API (1952), 383-390.
8. Mannon, R.W. and Chilingar, G.V.: "Experiment on Effect of Water Injection Rate on Imbibition Rate in Fractured Reservoirs," paper SPE 4101 presented at the 1972 Annual Fall Meeting of the SPE of AIME, San Antonio, Oct. 8-11.
9. Kleppe, J. and Morse, R.A.: "Oil production from Fractured Reservoirs by Water Displacement," paper SPE 5084 presented at the 1974 SPE Annual Meeting, Houston, Oct. 6-9.
10. Kazemi, H. and Merrill, L.S.: "Numerical Simulation of Water Imbibition in Fractured Cores," paper SPE 6895 presented at the 1977 SPE Annual Technical Conference and Exhibition, Denver, Oct. 9-12.
11. Babadagli, T.: "Injection Rate Controlled Capillary Imbibition Transfer in Fractured Systems," paper SPE 28640 presented at the 1994 SPE Annual Technical Conference and Exhibition, New Orleans, Sept. 25-28.
12. Guo, B. and Svec, R.: "A Preliminary Analysis of Permeabilities in the Teague-Blinbary Reservoir based on Step-Rate Test on Well Lamunyon Federal #62 and Whole Cores from Well Lamunyon Federal #50," PRRC internal report, January 29, 1998.
13. Seright, R., *et al.*: "Gel Placement Technique," unpublished manuscript, PRRC internal report (1996).
14. Kazemi, H., Merrill, L.S., Porterfield, L.K., and Zeman, P.R.: "Numerical Simulation of Water-Oil Flow in Naturally Fractured Reservoirs," *SPEJ* (Dec. 1976), 317-26.

Table 1—Core and Fluid Properties

Core Properties							**Fluid properties at 138°F**	
Cores #	Length, (cm)	Diam., (cm)	Perm. to brine, (md)	f, (%)	$S_{wi,}$ (%)	$S_{or,}$ (%)	m_o, (cp)	5.92
SPR-8H	6.487	3.608	0.17	10.98	34.04	57.03	m_w, (cp)	0.68
SPR-9H	6.502	3.607	0.33	10.26	41.29	49.90	r_o, (gr/cc)	0.850
SPR-10H	5.433	3.607	0.14	10.11	39.96	52.53	r_w, (gr/cc)	1.076
SPR-11H	5.842	3.607	0.10	10.71	40.55	51.62	IFT, (dyne/cm)	26.22

Table 2—Core and fluid properties for Berea core

Core Properties		**Fluid Properties**	
D (cm)	3.786	Oil	Spraberry oil
L (cm)	6.8936	Water	Spraberry brine
k_m (md)	28.09	m_o (cp)	3.52
f_m (%)	17.16	m_w (cp)	0.68
k_f (md)	3429	S_{wi} (%)	0
f_f (%)	1.0	S_{or} (%)	40
w_f (cm)	0.0076		

Table 3—Core and fluid properties for Spraberry core

Core Properties		**Fluid Properties**	
D (cm)	3.607	Oil	Spraberry oil
L (cm)	5.842	Water	Spraberry brine
k_m (md)	0.5	m_o (cp)	5.92
f_m (%)	10.84	m_w (cp)	0.68
k_f (md)	335	S_{wi} (%)	36.6
f_f (%)	1.0	S_{or} (%)	42.51
w_f (cm)	0.0024		

Table 4—Rock properties of Spraberry and Berea cores

	Spraberry Core		**Berea Core**	
Parameter	Lab unit	Field unit	Lab unit	Field unit
m_w	0.68	0.68	0.68	0.68
A	-	40	-	40
$L_{inj\text{-}prod}$	6.8	933.4	7.1	933.4
H	3.6	10	3.7	10
A_m	24.8	9333.81	25.807	9333.81
K	0.1	0.1	63.41	63.41
f	0.1	0.1	0.166	0.166
P_{cmax}	7	7	1.2	1.2
q	0	0	25	25
s	26.2	26.2	26.2	26.2
J	0.27	0.27	0.99	0.99
q_{crit}	10	393.22	20	1013.26
$Nfvc$	1.010^{-7}	-	2.8210^{-7}	-

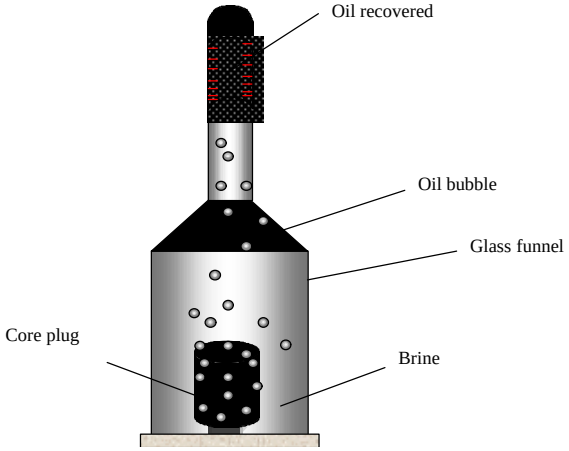

Fig. 1—Physical process of laboratory spontaneous imbibition.

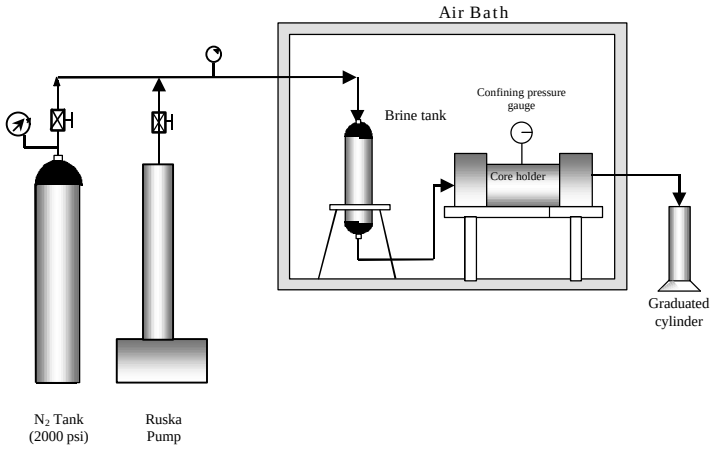

Fig. 3—Experimental setup of dynamic imbibition.

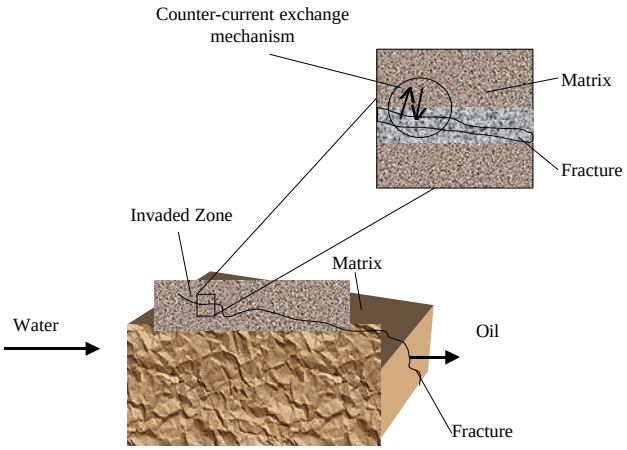

Fig. 2— Concept of dynamic imbibition process.

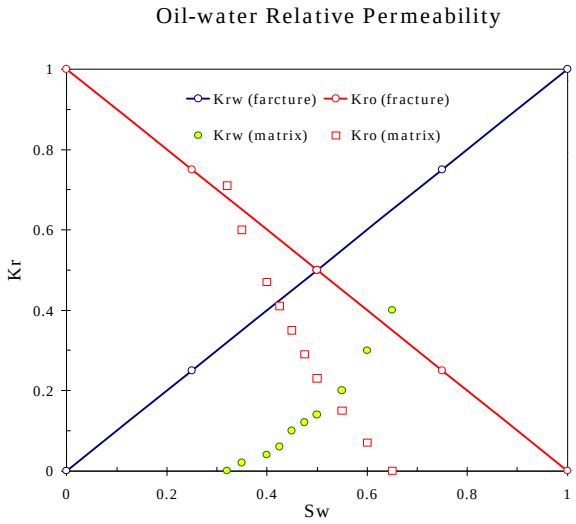

Fig. 4—Relative permeability curves.

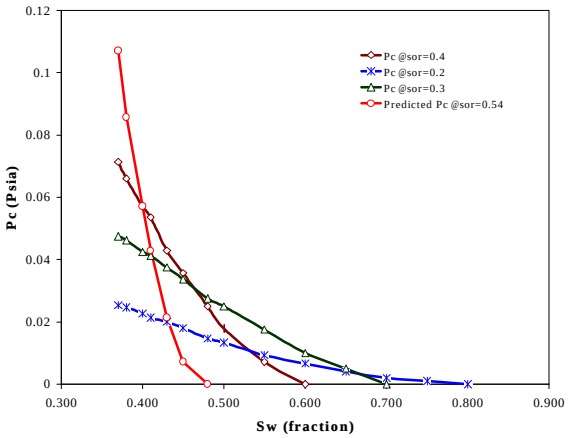

Fig. 5 —Imbibition capillary pressure obtained from matching spontaneous imbibition data.

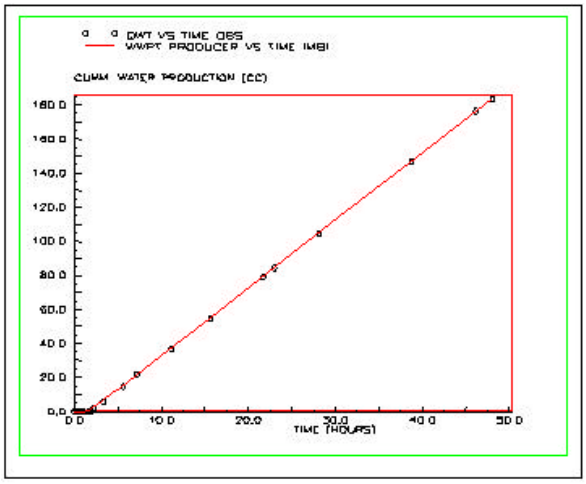

Fig. 7—Matching between experimental data and the numerical solution (Berea core - cumulative water production, injection rate = 4.0 cc/hr).

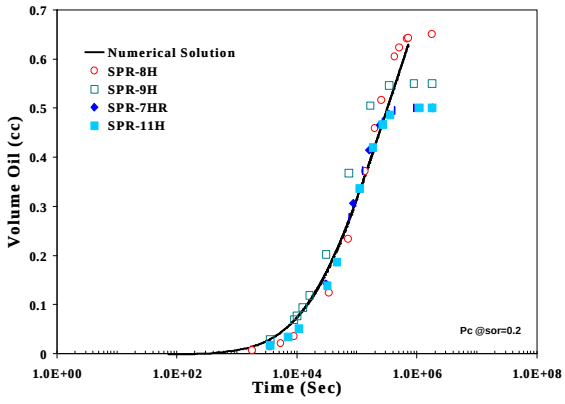

Fig. 6—Matching between spontaneous-imbibition experiments with numerical solution using 0.2 S_{or}.

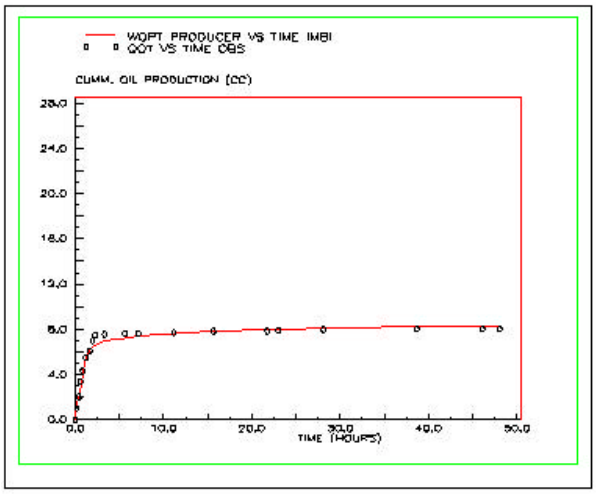

Fig. 8—Matching between experimental data and the numerical solution (Berea core - cumulative oil production, injection rate = 4.0 cc/hr).

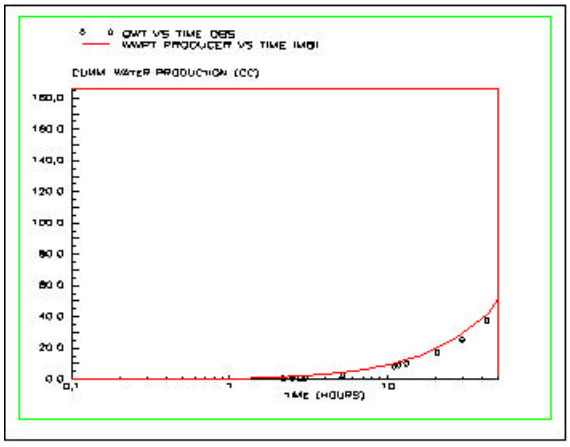

Fig. 9—Matching between experimental data and the numerical solution (Spraberry core - cumulative water production, injection rate = 1.0 cc/hr).

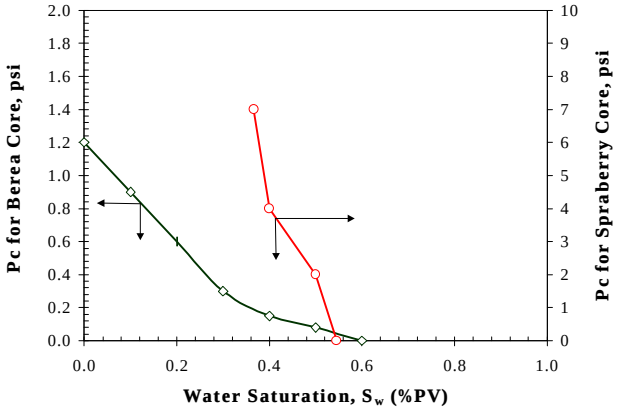

Fig. 11—Capillary pressure obtained as a result of matching experimental data (Berea and Spraberry cores).

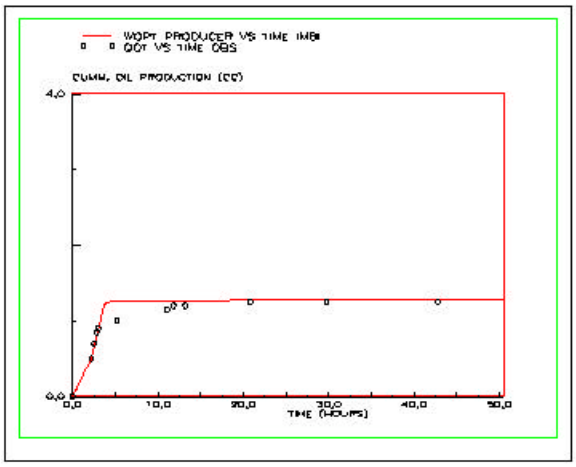

Fig. 10—Matching between experimental data and the numerical solution (Spraberry core - cumulative oil production, injection rate = 1.0 cc/hr).

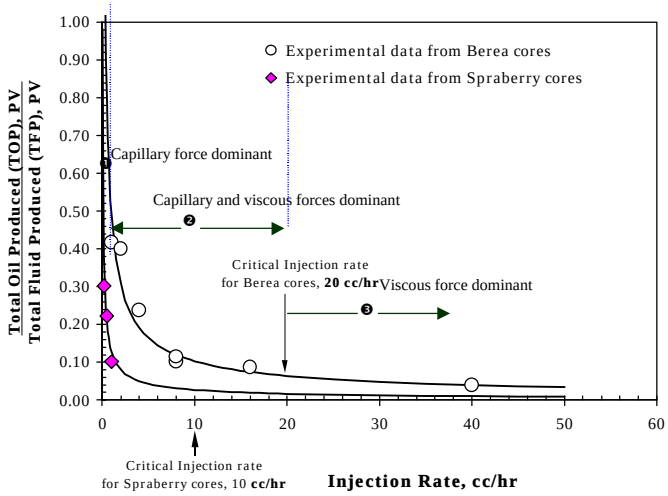

Fig. 12—Injection rate vs. oil cut (TOP/TFP).